

Engineering Notes

Minimum-Time Reorientation of Axisymmetric Rigid Spacecraft Using Three Controls

Elisha R. Pager and Anil V. Rao University of Florida, Gainesville, Florida 32611

https://doi.org/10.2514/1.A35422

I. Introduction

INIMUM-TIME rigid-body reorientation problems first gained traction in the work of Bilimoria and Wie [1], where a three-axis rigid-body spacecraft was considered and eigenaxis rotations were shown to not be time optimal. The work of Shen and Tsiotras [2] later showed that more generic time-optimal solutions could be obtained by considering axisymmetric rigid bodies controlled by two torques, i.e., an underactuated spacecraft. Shen and Tsiotras [2] and Tsiotras and Longuski [3] further advanced the work of Bilimoria and Wie [II] by extending the analysis from a triaxisymmetric body to an axisymmetric body, and highlighted the challenges associated with solving minimum-time reorientation problems. Despite these difficulties, the results of Refs. [2,3] have practical applications because many spacecraft can be modeled as an axisymmetric body instead of a triaxisymmetric rigid body. The results in Ref. [4] later showed that the time-optimal reorientation of an axisymmetric body could be extended to three control torques while still considering a spin-stabilized orientation, and solutions obtained for this three-torque control problem showed improvement over solutions obtained with the two-torque control model.

This paper revisits the minimum-time reorientation of a spinstabilized axisymmetric rigid spacecraft using three control torques. As alluded to earlier, the optimal solutions to such problems are known to have a control that is either bang-bang or singular [2,5]. This work analyzes the optimal solution structure of the minimumtime reorientation problem and discusses optimal solutions of various minimum-time maneuvers. Furthermore, numerical solutions are obtained using a recently developed bang-bang and singular optimal control (BBSOC) method, which solves bang-bang and singular optimal control problems [5].

Although both Ref. [2] and this work focus on the optimization of a minimum-time axisymmetric rigid spacecraft, the work in this paper differs significantly from the work of Shen and Tsiotras [2] in the following ways. First, the numerical approach used to solve the problem in Ref. [2] consisted of using an indirect shooting method that required the formulation of the optimality conditions, whereas in this work the aforementioned direct collocation BBSOC method [5] is employed. This difference in methodology is significant because the BBSOC method does not require a priori information about the

Received 16 March 2022; revision received 15 June 2022; accepted for publication 17 June 2022; published online 8 August 2022. Copyright © 2022 by Elisha Rose Pager and Anil Vithala Rao. Published by the American Institute of Aeronautics and Astronautics, Inc., with permission. All requests for copying and permission to reprint should be submitted to CCC at www copyright.com; employ the eISSN 1533-6794 to initiate your request. See also AIAA Rights and Permissions www.aiaa.org/randp.

solution structure or optimality conditions. Also, as stated, the BBSOC method is implemented using a multiple-domain Legendre—Gauss—Radau (LGR) direct collocation method [5], where a convergence theory has been established under certain assumptions on smoothness and coercivity [7]. Next, the BBSOC method produced more accurate solutions to the problem under consideration relative to the numerical solutions obtained in Ref. [2]. Finally, as first observed in Ref. [4], three control torques are considered in this paper, whereas only two control torques were considered in Ref. [2]. The inclusion of a third control torque produces smaller optimal terminal times because the third control torque makes it possible to optimize the rotation of the body about the axis of symmetry and, thus, allowing the body to spin about its symmetry axis at a nonconstant rate.

The remainder of the paper is organized as follows. Section presents the system model and problem formulation studied. Section presents the optimality conditions derived from Pontryagin's minimum principle along with a brief analysis of the singular controls. Section very provides an overview of the numerical approach used to solve the problem, the BBSOC method, and the numerical approach developed in Ref. 2. Section very provides numerical results for three different maneuvers studied. The results are then summarized and further discussed in Sec. very provides conclusions on this research.

II. Formulation of Optimal Control Problem

The minimum-time reorientation of an axisymmetric rigid space-craft shown in Fig. [] is stated as follows: Minimize

$$J = t_f \tag{1}$$

subject to the dynamic constraints

$$\dot{\omega}_{1} = a\omega_{3}\omega_{2} + u_{1},
\dot{\omega}_{2} = -a\omega_{3}\omega_{1} + u_{2},
\dot{\omega}_{3} = u_{3},
\dot{x}_{1} = \omega_{3}x_{2} + \omega_{2}x_{1}x_{2} + \frac{\omega_{1}}{2}(1 + x_{1}^{2} - x_{2}^{2}),
\dot{x}_{2} = -\omega_{3}x_{1} + \omega_{1}x_{1}x_{2} + \frac{\omega_{2}}{2}(1 + x_{2}^{2} - x_{1}^{2})$$
(2)

the control path constraints

$$u_{\min} \le u_j \le u_{\max}, \quad j \in (1, 2, 3)$$
 (3)

and the boundary conditions

$$\boldsymbol{\omega}(0) = [\omega_{10}, \omega_{20}, \omega_{30}]^{\mathsf{T}},$$

$$\boldsymbol{x}(0) = [x_{10}, x_{20}]^{\mathsf{T}},$$

$$\boldsymbol{\Phi}[\boldsymbol{Y}(t_f)] = \boldsymbol{0}$$
(4)

where $\omega = (\omega_1, \omega_2, \omega_3)$ is the angular velocity, $\mathbf{x} = (x_1, x_2)$ is the relative position of the inertially fixed "3"-axis as viewed by an observer fixed in the body $[\mathbf{B}]$, $\mathbf{Y} = [\boldsymbol{\omega}, \mathbf{x}]$ is the state, $\mathbf{u} = (u_1, u_2)$ is the control, (I_1, I_2, I_3) are the principal-axis moments of inertia, $a = (I_2 - I_3)/I_1$, and $\Phi : \mathbb{R}^5 \to \mathbb{R}^k$, $k \le 5$ is a differentiable vector function that defines the terminal constraints on the state. Further details on the model and associated derivations are found in Ref. $[\mathbf{R}]$.

^{*}Ph.D. Candidate, Department of Mechanical and Aerospace Engineering; epager@ufl.edu.

[†]Professor, Department of Mechanical and Aerospace Engineering; anilyrao@ufl.edu (Corresponding Author).

III. Mathematical Analysis

The Hamiltonian for the optimal control problem defined in Sec. \blacksquare is given as

$$\mathcal{H} = \lambda_1 (a\omega_3\omega_2 + u_1) + \lambda_2 (-a\omega_3\omega_1 + u_2) + \lambda_3 u_3$$

$$+ \lambda_4 \Big(\omega_3 x_2 + \omega_2 x_1 x_2 + \frac{\omega_1}{2} (1 + x_1^2 - x_2^2) \Big)$$

$$+ \lambda_5 \Big(-\omega_3 x_1 + \omega_1 x_1 x_2 + \frac{\omega_2}{2} (1 + x_2^2 - x_1^2) \Big)$$
 (5)

where $\lambda=(\lambda_1,\lambda_2,\lambda_3,\lambda_4,\lambda_5)$ is the costate. The remaining first-order necessary conditions are

$$\dot{\lambda} = -\left[\frac{\partial \mathcal{H}}{\partial Y}\right]^{\mathsf{T}},$$

$$\lambda^{\mathsf{T}}(t_f) = \nu^{\mathsf{T}} \frac{\partial \Phi}{\partial Y(t_f)},$$

$$\mathcal{H}(t_f) = -1 \tag{6}$$

where $\nu \in \mathbb{R}^k$. Because the control appears linearly in the Hamiltonian, the optimal control is obtained from Pontryagin's minimum principle as

$$u_{j}^{*} = \begin{cases} u_{\min}, & g_{j} > 0, \\ u_{j,s}, & g_{j} = 0, & j \in (1, 2, 3) \\ u_{\max}, & g_{j} < 0, \end{cases}$$
 (7)

where

$$g_j = \lambda_j, \qquad j \in (1, 2, 3) \tag{8}$$

are the switching functions corresponding to the components u_j , $j \in (1, 2, 3)$, of the control, respectively.

A. Singular Control Analysis

Assume now that $a \neq 0$ and $\omega_3 \neq 0$, $\forall t \in [t_0, t_f]$. An optimal control component u_j^* is singular whenever $g_j = 0$ during a nonzero interval $[t_1, t_2] \subset [t_0, t_f]$ and is obtained from the condition

$$\frac{d^{(2r_j)}}{dt^{(2r_j)}}(g_j) = 0, \qquad (r_j = 0, 1, 2, \dots), \qquad j = 1, 2, 3$$
 (9)

where $2r_j$ is the minimum number of times g_j is differentiated to obtain the corresponding control $u_{j,s}$ [2, \square]. Furthermore, the generalized Legendre–Clebsch condition [2, \square , \square]

$$(-1)^r \frac{\partial}{\partial u_i} \left[\frac{d^{2r}}{dt^{(2r)}} g_j \right] \ge 0, (r_j = 0, 1, 2, ...), j = 1, 2, 3$$
 (10)

must hold over the duration of a singular arc $[t_1, t_2]$. Finally, because Shen and Tsiotras [2] showed that it is suboptimal for all three control components to be singular, this paper considers the case where only one control component is singular along with the two special cases where either a or ω_3 is zero.

B. Special Cases

First, for the case where one of the first two control components is singular while the other two control components are bang-bang, the switching function of interest must be differentiated with respect to time *four* times until the corresponding control component appears [8]. The singular control components $u_{1,s}$ and $u_{2,s}$ are then given as follows:

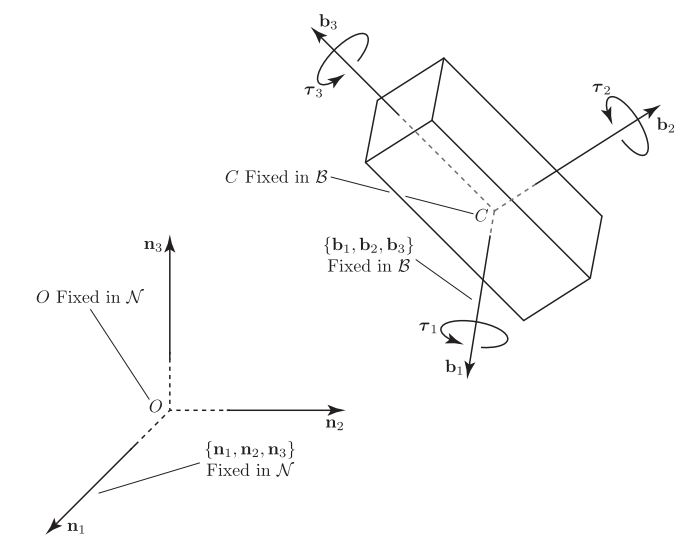


Fig. 1 Axisymmetric rigid body with three control torques.

The remaining bang-bang control components are determined according to Eq. (1). Furthermore, the generalized Legendre–Clebsch condition in Eq. (10) implies that the denominator of Eqs. (11) and (12) must be nonnegative in order for the singular control to be optimal.

Next, for the case where $\omega_3 \equiv 0$ the control component u_3 is eliminated from Eq. (2), u_1 is singular, and u_2 is bang-bang such that [8]

$$u_{1s}^* = 0 (13)$$

and

$$u_2^* = \begin{cases} u_{2,\min}, & \lambda_2 > 0, \\ u_{2,\max}, & \lambda_2 < 0 \end{cases}$$
 (14)

Finally, for the special case when a=0 and ω_3 is constant, u_3 is eliminated, u_1 singular, and u_2 bang-bang. Moreover, because all higher-order derivatives of g_1 are zero, u_1 lies on an infinite-order singular arc. Consequently, any value of u_1 that lies within the limits $[u_{1,\min}, u_{1,\max}]$ and satisfies the boundary conditions is optimal, while the bang-bang control u_2 is determined by Eq. (14).

IV. Numerical Approach: BBSOC Method

The optimal control problem formulated in Sec. [] is solved using the BBSOC method developed in Ref. [6]. The BBSOC method identifies the existence of singular arcs in the optimal control and then performs an iterative regularization procedure on an interval where a singular control has been identified. The BBSOC method also identifies the switching structure of a nonsmooth control solution and optimizes the values of the switch times. After the bangbang and singular structure has been identified, the BBSOC method performs a multiple-domain partitioning of the original domain such that each domain corresponds to one of the identified behaviors in the optimal control. The method is algorithmic in nature and requires no user input. A flowchart for the BBSOC method is provided in Fig. [2]. More details on the BBSOC method and the multiple-domain LGR collocation can be found in Refs. [5].

$$u_{1,s} = -\frac{\dot{\lambda}_2[2a\omega_3^3(a+1)^2 - 2a\omega_3\omega_1^2 + 2a\omega_3\omega_2^2 + 2\omega_1u_2] - \omega_2\lambda_2(4a^2\omega_3^2\omega_1 - 3a\omega_3u_2)}{\dot{\lambda}_2\omega_2 - \omega_3(1+2a)(\lambda_3x_2 - \lambda_4x_1)}$$
(11)

$$u_{2,s} = -\frac{\dot{\lambda}_1 [2a\omega_3^3(a+1)^2 - 2a\omega_3\omega_1^2 + 2a\omega_3\omega_2^2 + 2\omega_2u_1] - \omega_1\lambda_1(4a^2\omega_3^2\omega_2 + 3a\omega_3u_1)}{\dot{\lambda}_1\omega_1 - \omega_3(1+2a)(\lambda_3x_2 - \lambda_4x_1)}$$
(12)

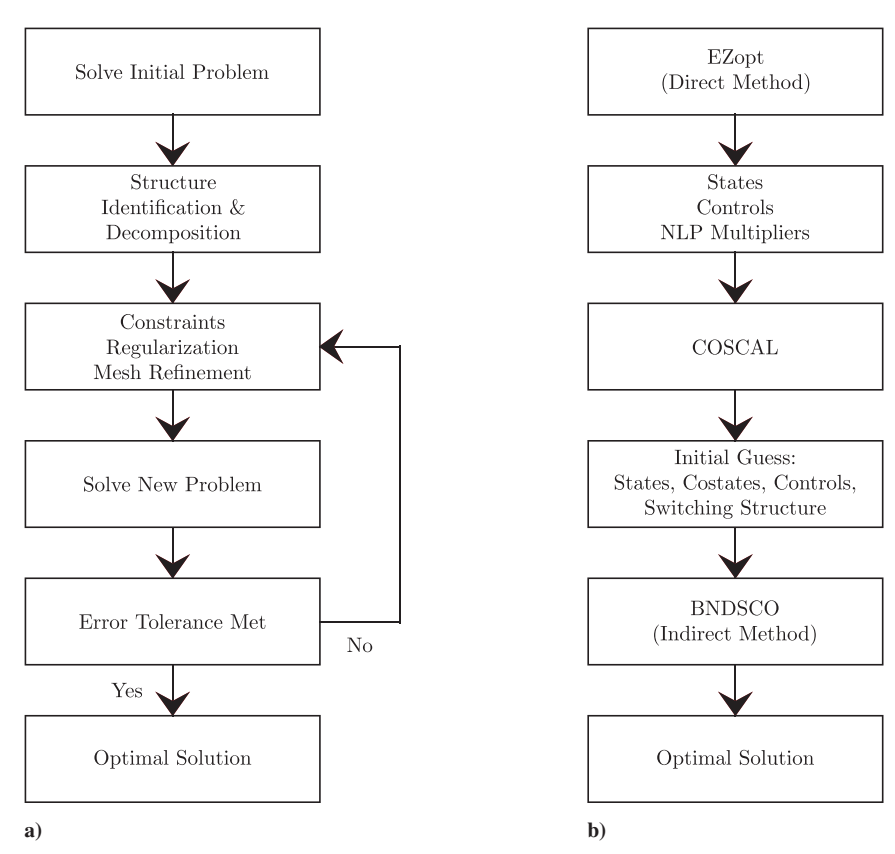


Fig. 2 Flowchart of the a) BBSOC method and b) computational scheme used in Ref. [2].

An important contribution of this paper is comparing the approach used in this paper with the approach used in Ref. [2]. Specifically, the BBSOC method has been developed for solving nonsmooth and singular optimal control problems. In this paper, the performance of the BBSOC method is compared to the approach used in Ref. [2]. Specifically, the method of Shen and Tsiotras [2] uses an indirect shooting method to solve the optimal control problem. Given that a very good initial guess is often required in order to successfully employ an indirect method, Shen and Tsiotras [2] first uses a direct method, EZopt, to obtain an initial guess for the indirect method, BNDSCO, a multiple-shooting based optimal control software. In particular, the Lagrange multipliers obtained from EZopt are used to obtain initial guesses for the costates using COSCAL, a costate calculator developed in Ref. [2]. Then, an initial guess of the states, costates, and controls along with the switching structure is provided to BNDSCO. Given that Shen and Tsiotras [2] employ an indirect shooting method, the higher-order singular optimality conditions must be derived and the switching structure of the control must be known a priori. On the other hand, the BBSOC method used to generate the results in this paper neither requires that the higher-order singular arc optimality conditions be derived nor does it require a priori knowledge of the switching structure of the optimal control. Instead, the BBSOC method identifies algorithmically the structure of the optimal control and solves for the singular control through the aforementioned regularization procedure (which is itself algorithmic and requires no user intervention). Figure 2 provides a flowchart that compares the BBSOC method to the method of Shen and Tsiotras [2].

V. Results

All results presented in this section were obtained using the BBSOC method [δ] implemented in MATLAB® with the nonlinear programming (NLP) problem solver IPOPT [δ], where IPOPT was employed in full-Newton (second-derivative) mode using the default NLP solver tolerance of $\epsilon_{\rm NLP}=10^{-7}$. Any necessary mesh refinement was performed using the mesh refinement method described in Ref. [δ] using a mesh refinement accuracy tolerance of $\epsilon_{\rm mesh}=10^{-1}$

10⁻⁵ along with a minimum and maximum number of LGR points in each interval of 3 and 12, respectively. The BBSOC method was initialized using a mesh that consisted of 20 uniformly spaced mesh intervals and three collocation points per mesh interval. A straight-line guess is used for variables with boundary conditions at both endpoints, and a constant guess is used for variables with boundary conditions at only one endpoint. All derivatives required by IPOPT were provided using the algorithmic differentiation software *ADi-Gator* [16]. Finally, all computations were performed on a 2.9 GHz 6-Core Intel Core i9 MacBook Pro running Mac OS Big Sur Version 11.6 with 32 GB 2400 MHz DDR4 of RAM, using MATLAB version R2019b (build 9.7.0.1190202), and all computation (CPU) times are in reference to this aforementioned machine.

The following three maneuvers are considered: 1) a rest-to-rest (RTR) maneuver, where the resulting control is bang-bang; 2) a nonrest-to-rest (NRTR) nonspinning maneuver, where the resulting control exhibits a finite-order singular arc; and 3) a rest-to-nonrest (RTNR) maneuver, where the resulting control exhibits an infinite-order singular arc. Each case is solved using the BBSOC method and $\mathbb{CPOPS} - \mathbb{H}$ [17] (referred to as hp-LGR in Discussion), and also compared with the results presented in Ref. [2], where the numerical approach discussed in Sec. [7] is implemented.

A. Rest-to-Rest Maneuver: Bang-Bang Control

The RTR maneuver assumes that both a and ω_3 are nonzero and a = 0.5. The boundary conditions for this case are given as

$$\omega_{10} = 0,$$
 $\omega_{1f} = 0,$
 $\omega_{20} = 0,$ $\omega_{2f} = 0,$
 $\omega_{30} = -0.5,$ $\omega_{3f} = -0.5,$
 $x_{10} = 1.5,$ $x_{1f} = 0,$
 $x_{20} = -0.5,$ $x_{2f} = 0$

For this maneuver, most RTR maneuvers, and some NRTR maneuvers where the body is spinning and axisymmetric, all three controls

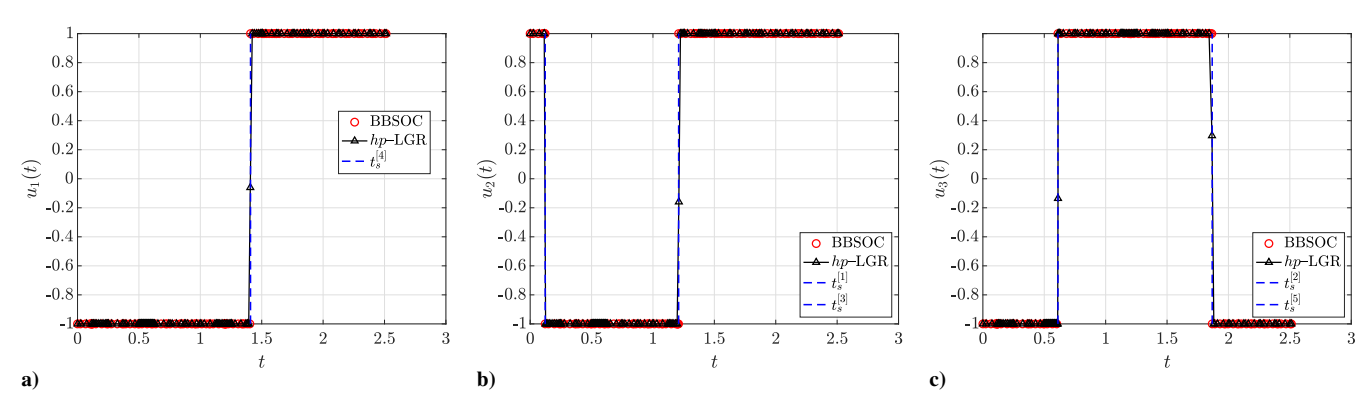


Fig. 3 Control component solutions for the spinning RTR maneuver.

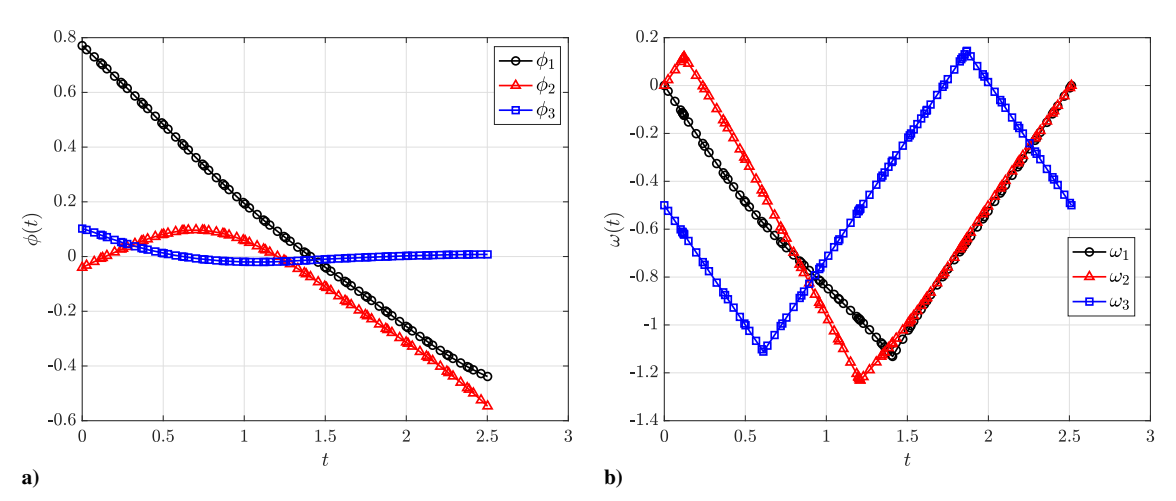


Fig. 4 Switching functions and state solutions for the spinning RTR maneuver.

are bang-bang [2]. The goal is to rotate the body until the direction of the symmetry axis is aligned with the inertially fixed 3-axis representing a rest condition. The three components of the optimal control were found to be bang-bang such that u_1 contains a single switch while u_2 and u_3 contain two switches. The minimum time to complete the maneuver was approximately 2.5126 s.

Figures 3 and 4 show the three control solutions along with their corresponding switching functions and time history of the angular velocities. It is observed in Fig. B that the BBSOC method identified the five switch times and constrained the control to the appropriate limit. In contrast, the solution obtained using the hp-LGR method contains collocation points located between the lower and upper limits on the control in the neighborhood of the switch times. Table provides a further comparison between the BBSOC and hp-LGR methods by showing the performance of each method and by comparing the values of the switch points and the minimum terminal time. Table I also compares the results of Shen and Tsiotras [2], where it is seen that the BBSOC method not only obtains a lower optimal terminal time, but also obtains the solution in a more computationally efficient manner than the method of Shen and Tsiotras [2]. It is noted that Shen and Tsiotras [2] claimed that it took less than 2 s for BNDSCO to converge. Note, however, that it took EZopt 2 minutes to converge to the initial guess required as the initial guess for BNDSCO. As a result, it is seen that one of the major drawbacks

Table 1 Comparison of computational results for the RTR maneuver

Method	$t_s^{[1]}$	$t_s^{[2]}$	$t_s^{[3]}$	$t_s^{[4]}$	$t_s^{[5]}$	t_f	CPU, s
BBSOC	0.1224	0.6114	1.2091	1.4088	1.8676	2.5126	2.09
hp-LGR	0.1145	0.6118	1.2108	1.4069	1.8658	2.5126	4.41
Ref. [2]						2.61	122

of using an indirect method beyond requiring the derivation of the singular optimality conditions is increased computation time relative to a direct collocation method such as the BBSOC method. Furthermore, by allowing the symmetry axis to spin at a nonconstant rate, a smaller terminal time is achieved by the three-torque control formulation used in this paper as compared to the two-torque formulation in Ref. [2]. Specifically, Table [1] shows a 3.73% reduction in the terminal time obtained by the BBSOC method compared with the method of Shen and Tsiotras [2].

B. Nonrest-to-Rest Maneuver for $\omega_3 = 0$: Finite Singular Arc

For this special case the body is assumed not to be spinning about the symmetry axis. Therefore, $(a, \omega_3) = (0.5, 0)$, $\forall t \in [t_0, t_f]$ and the boundary conditions are given as

$$\omega_{10} = -0.45, \quad \omega_{1f} = 0,$$
 $\omega_{20} = -1.1, \quad \omega_{2f} = 0,$
 $\omega_{30} = 0, \quad \omega_{3f} = 0,$
 $x_{10} = 0.1, \quad x_{1f} = 0,$
 $x_{20} = -0.1, \quad x_{2f} = 0$

An analysis of this special case has been provided in Sec. III. and showed that the first control component contains a second-order singular arc [as given in Eq. ([3])] while the second control component is bang-bang. The optimal minimum time to complete the maneuver is 2.8839 s.

Figures \boxed{a} , \boxed{b} , and \boxed{a} show the optimal controls and switching functions obtained using the BBSOC method and hp-LGR method. The singular arc begins at $t_s^{[4]} \approx 1.9054$. A numerical issue that occurs when using direct methods on singular optimal control problems is the

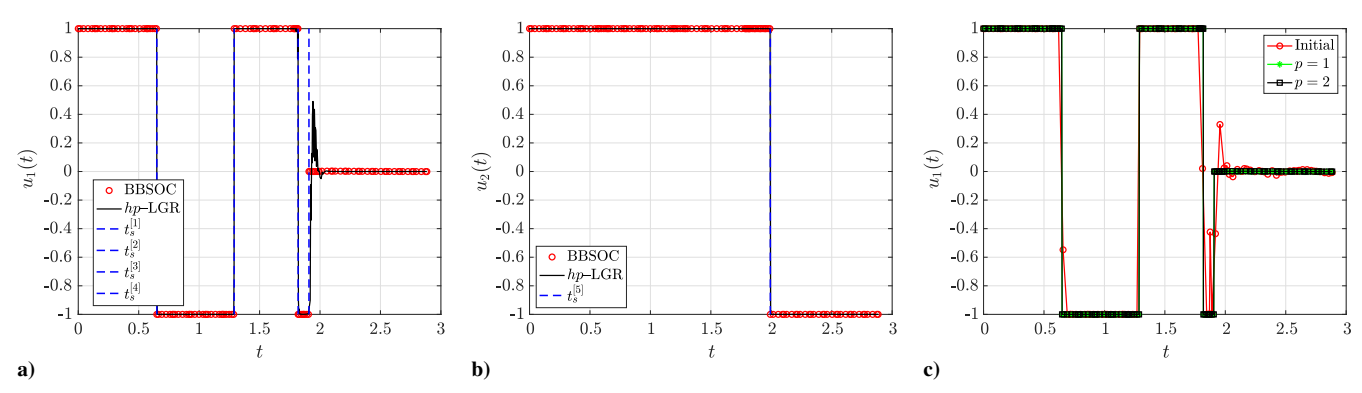


Fig. 5 Control component solutions for the nonspinning NRTR maneuver, where Fig. 5c shows the control history of the BBSOC method for obtaining the singular control.

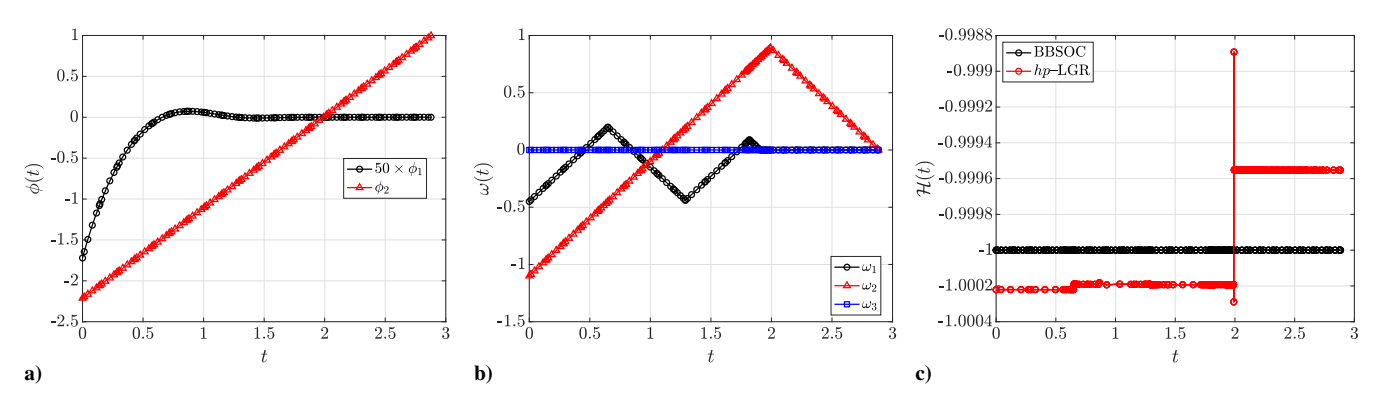


Fig. 6 Switching functions and state solutions for the nonspinning NRTR maneuver, where Fig. 6 shows the time history of the Hamiltonian.

Table 2 Comparison of computational results for the nonspinning NRTR maneuver

Method	$t_s^{[1]}$	$t_s^{[2]}$	$t_s^{[3]}$	$t_s^{[4]}$	$t_s^{[5]}$	t_f	δ	ϵ	p	CPU, s
BBSOC	0.6498	1.2898	1.8177	1.9054	1.9919	2.8839	1.24×10^{-10}	10^{-3}	2	3.37
hp-LGR	0.6498	1.2897	1.8184	1.9226	1.9922	2.8839				5.18
Ref. [2]				1.9040		2.8800		——		302

occurrence of chattering behavior along the singular arc. This is observed in the hp-LGR solution and successfully removed by the BBSOC method as shown in Fig. Σ . Figure Σ shows the control history of the regularization procedure implemented by the BBSOC method. Additionally, values for the switch times and final time are provided in Table 2 along with the CPU times for each method. Given that Shen and Tsiotras [2] do not provide the final time for their solution to more than two decimal places, it is difficult to compare the minimum times achieved by each of the numerical approaches. It is also noted that the CPU time listed for Ref. [2] is composed of the time it took for EZopt to converge to the initial guess for BNDSCO (5 minutes) and the computation time for BNDSCO (2 s). Regardless, it is clear that the

BBSOC framework is more computationally efficient at solving nonsmooth and singular optimal control problems.

Optimality is verified for the existence of the singular arc by checking that the generalized Legendre-Clebsch condition in Eq. ([1]) is satisfied and checking that the Hamiltonian satisfies the transversality condition in the last line of Eq. ([5]). According to Pager and Rao [[8]], $\omega_1 = x_1 = 0$ for Eq. ([1]0) has to be satisfied. This is confirmed by looking at ω_1 and x_1 in Figs. [5]5 and [7]6. The second point can be verified by computing the Hamiltonian using the numerical solution obtained by each method. The Hamiltonian time history is provided in Fig. [5]6 and shows that the BBSOC solution is optimal by producing a constant Hamiltonian value of -1, whereas

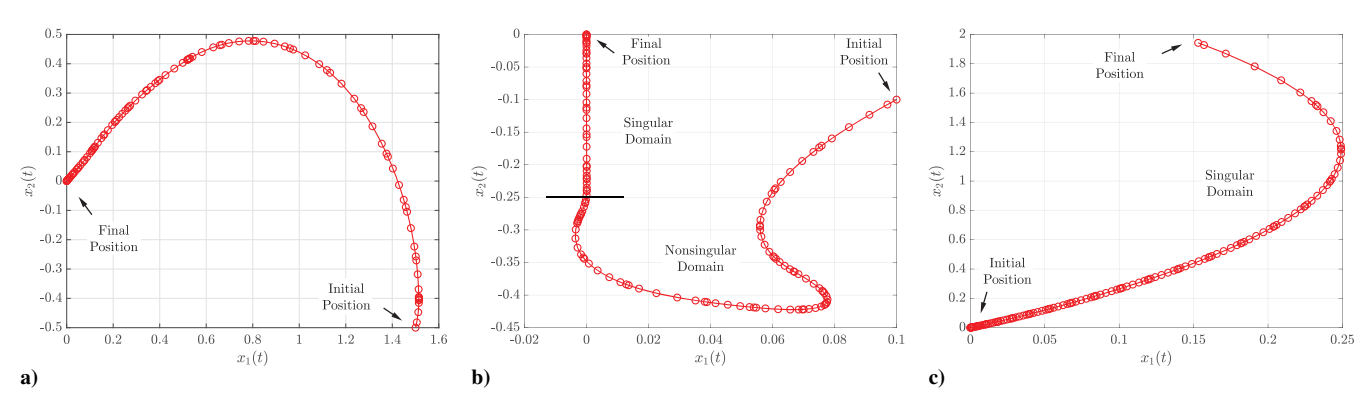


Fig. 7 Optimal trajectories for the a) RTR, b) nonspinning NRTR, and c) inertially symmetric RTNR maneuvers in the x_1-x_2 plane.

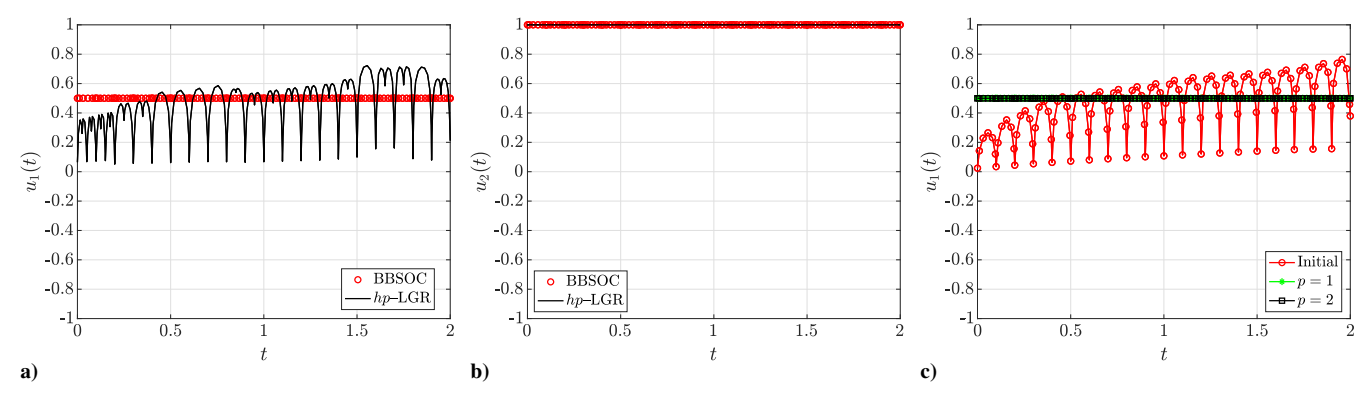


Fig. 8 Control component solutions for the inertially symmetric RTNR maneuver, where Fig. 5c shows the control history of the BBSOC method for obtaining the singular control.

the hp-LGR solution produces a nonconstant Hamiltonian. The maximum absolute error of the Hamiltonian for both the BBSOC method and the hp-LGR method is 1.69×10^{-7} and 1.11×10^{-3} , respectively. The singular control produced by the BBSOC method can also be compared with the optimal control law in Eq. ([3]), where the maximum absolute error is 1.3×10^{-5} . Thus, the singular arc is optimal based on the analysis of Sec. [1] and the optimality verification provided in this section.

C. Rest-to-Nonrest Maneuver for a = 0: Infinite-Order Singular Arc

For this special case the rigid body is assumed to be inertially symmetric but spinning at a constant rate about the symmetry axis. Consequently, a = 0 and the boundary conditions are given as

$$\omega_{10} = 0,$$
 $\omega_{1f} = 1,$
 $\omega_{20} = 0,$ $\omega_{2f} = 2,$
 $\omega_{30} = -0.3,$ $\omega_{3f} = -0.3,$
 $x_{10} = 0,$ $x_{1f} = \text{Free},$
 $x_{20} = 0,$ $x_{2f} = \text{Free}$

Table 3 Comparison of computational results for the spinning inertially symmetric RTNR maneuver

Method	\mathcal{J}^*	δ	ϵ	p	CPU, s	
BBSOC	2.00	1.11×10^{-19}	10^{-1}	2	1.77	
hp-LGR	2.00				1.74	
Ref. [2]	2.00		——			

and represent an RTNR maneuver. The first control component contains an infinite-order singular arc across the entire time horizon, the second component is bang-bang, and the third control component is zero since ω_3 is constant. As a result of the infinite-order singular arc, many singular control solutions produce the optimal trajectory. The fact that many singular solutions exist is explained by looking at the reduced dynamics where it is noted that ω_2 must reach the specified final angular velocity of 2 rad/s in 2 s (which is the optimal final time). One solution to the infinite-order singular arc is provided in Fig. 8a. Likewise, the corresponding numerical solution is provided in Figs. 86 and 96 including the second control component, the regularization iteration history for the singular control component, the corresponding control switching functions, and time histories of angular velocity. As expected, these results are in agreement with the results of Shen and Tsiotras [2] (see Table 3), noting that the results of this work were obtained without using the known structure of control or the fact that the control lies on an infinite-order singular arc. The parameters associated with the BBSOC method are provided in Table β along with the CPU times for the BBSOC and hp-LGR methods.

Finally, optimality can be verified for the occurrence of the singular arc by checking that the boundary conditions are satisfied and checking that the Hamiltonian satisfies the transversality condition in the last line of Eq. (6). The first point is verified by checking the state solution. The second point can again be verified by calculating the Hamiltonian using the numerical solution obtained by each method. The Hamiltonian time history is analyzed and shows that the maximum absolute error of the Hamiltonian for both the BBSOC method and the hp-LGR method is 9.99×10^{-9} and 1.61×10^{-8} , respectively. Thus, the infinite-order singular arc is optimal based on the analysis of Sec. III.A and the optimality verification provided in this section.

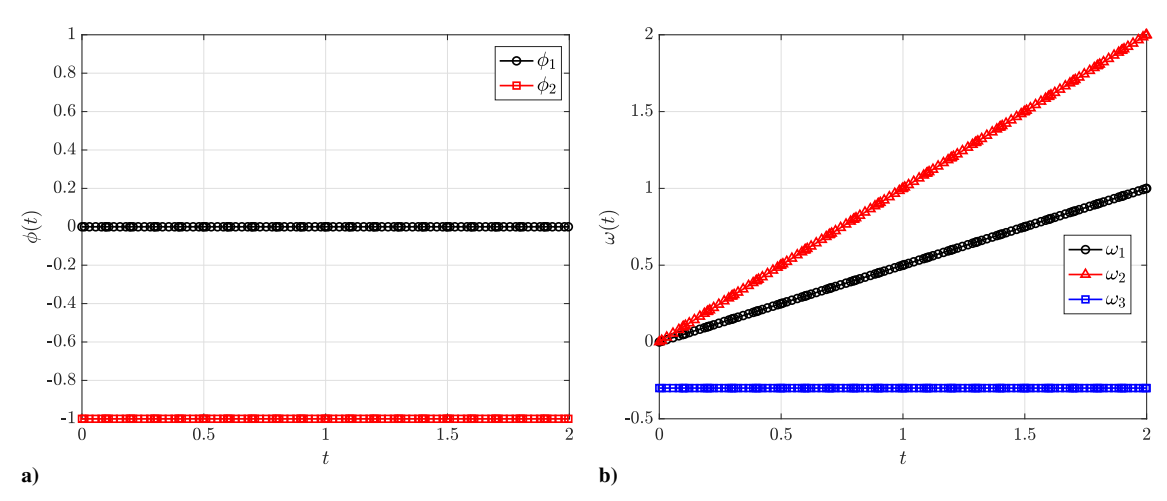


Fig. 9 Switching functions and state solutions for the inertially symmetric RTNR maneuver.

VI. Discussion

It is seen for the three maneuvers studied in Sec. It that the BBSOC method outperforms the method of Shen and Tsiotras [2] both in computation time and in accuracy. Moreover, unlike the method of Shen and Tsiotras [2], the BBSOC method does not require that the singular arc conditions be derived and enforced. Furthermore, the BBSOC method neither requires accurate initial guesses of the solution nor requires a guess of the switching structure. In contrast, the results of the method in Ref. [2] are only obtained if BNDSCO is provided a near-optimal initial guess and the singular arc conditions are provided.

For the special case maneuvers described in Secs. $\[\]$ B and $\[\]$ the Hamiltonian was found to be numerically equal to -1 while the generalized Legendre–Clebsch condition (10) was satisfied for both singular controls. The hp-LGR and BBSOC methods produced errors in the Hamiltonian on the order of 10^{-3} and 10^{-8} , respectively. Finally, it was found for the bang-bang RTR maneuver that the errors in the Hamiltonian were 1.50×10^{-6} and 1.98×10^{-3} using the BBSOC and hp-LGR methods, respectively.

Finally, the optimal trajectories for each maneuver are discussed. Figure $\centsuremath{\mathbb{Z}}$ shows the optimal trajectories of each maneuver in the x_1-x_2 plane representing the goal of reorienting the relative position of the inertial 3-axis, with respect to the body-fixed frame, from an initial position to a final position. In particular, Fig. $\centsuremath{\mathbb{Z}}$ shows the trajectory for the NRTR maneuver when $\entsuremath{\omega}_3 = 0$ in Sec. $\centsuremath{\mathbb{Z}}$. Here the straight-line portion of the trajectory represents an eigenaxis rotation when the rigid spacecraft is not spinning about the symmetry axis. An eigenaxis rotation does not appear in any of the other solutions since eigenaxis rotations in general are not time optimal as shown in Refs. $\centsuremath{\mathbb{Z}}$, but they do often produce the shortest angular trajectory between the current attitude and the desired attitude. For this special case, however, the singular control is equivalent to an eigenaxis rotation along that portion of the trajectory and is optimal.

VII. Conclusions

The minimum-time reorientation of an axisymmetric rigid spacecraft under the influence of three control torques has been revisited. Different maneuvers, including special cases, have been considered and analyzed using a recently developed BBSOC method. It was found for the results obtained in this paper that the BBSOC method is both more efficient and more accurate than previously obtained results and without the need to derive and enforce the singular optimal control conditions. Finally, the results show that considering a three-torque control leads to smaller terminal times when compared with a two-torque control.

Acknowledgments

The authors gratefully acknowledge support for this research from the U.S. National Science Foundation under grant CMMI-2031213, the U.S. Office of Naval Research under grant N00014-19-1-2543, and from the U.S. Air Force Research Laboratory under contract FA8651-21-F-1041.

References

- [1] Bilimoria, K. D., and Wie, B., "Time-Optimal Three-Axis Reorientation of a Rigid Spacecraft," *Journal of Guidance, Control, and Dynamics*, Vol. 16, No. 3, 1993, pp. 446–452. https://doi.org/10.2514/3.21030
- [2] Shen, H., and Tsiotras, P., "Time-Optimal Control of Axisymmetric Rigid Spacecraft Using Two Controls," *Journal of Guidance, Control, and Dynamics*, Vol. 22, No. 5, Sept. 1999, pp. 682–694. https://doi.org/10.2514/2.4436

- [3] Tsiotras, P., and Longuski, J. M., "A New Parameterization of the Attitude Kinematics," *Journal of the Astronautical Sciences*, Vol. 43, No. 3, July–Sept. 1995, pp. 243–262.
- [4] Fleming, A., and Ross, I. M., "Optimal Control of Spinning Axisymmetric Spacecraft: A Pseudospectral Approach," AIAA Guidance, Navigation and Control Conference and Exhibit, AIAA Paper 2008-7164, June 2008. https://doi.org/10.2514/6.2008-7164
- [5] Seywald, H., and Kumar, R. R., "Singular Control in Minimum Time Spacecraft Reorientation," *Journal of Guidance, Control, and Dynamics*, Vol. 16, No. 4, July 1993, pp. 686–694. https://doi.org/10.2514/3.56607
- [6] Pager, E. R., and Rao, A. V., "Method for Solving Bang-Bang and Singular Optimal Control Problems Using Adaptive Radau Collocation," *Computational Optimization and Applications*, Vol. 81, No. 3, April 2022, pp. 857–887. https://doi.org/10.1007/s10589-022-00350-6
- [7] Hager, W. W., Hou, H., Mohapatra, S., Rao, A. V., and Wang, X.-S., "Convergence Rate for a Radau hp Collocation Method Applied to Constrained Optimal Control," *Computational Optimization and Appli*cations, Vol. 74, No. 1, 2019, pp. 274–314. https://doi.org/10.1007/s10589-019-00100-1
- [8] Pager, E. R., and Rao, A. V., "Minimum-Time Reorientation of Axisymmetric Rigid Spacecraft Using Three Controls," arXiv:2203. 11394, 2022. https://arxiv.org/abs/2203.11394.
- [9] Bryson, A. E., and Ho, Y., Applied Optimal Control: Optimization, Estimation, and Control, Hemisphere Publishing Corp., New York, 1975, Chap. 8.
- [10] Schättler, H., and Ledzewicz, U., Geometric Optimal Control: Theory, Methods and Examples, Vol. 38, Springer Science & Business Media, New York, 2012, Chap. 2.
- [11] Robbins, H. M., "A Generalized Legendre-Clebsch Condition for the Singular Cases of Optimal Control," *IBM Journal of Research and Development*, Vol. 11, No. 4, July 1967, pp. 361–372. https://doi.org/10.1147/rd.114.0361
- [12] Kopp, R. E., and Moyer, H. G., "Necessary Conditions for Singular Extremals," AIAA Journal, Vol. 3, No. 8, Aug. 1965, pp. 1439–1444. https://doi.org/10/2514/3.3165
- [13] Pager, E. R., and Rao, A. V., "Structure Identification Method for Nonsmooth and Singular Optimal Control Problems," AIAA Scitech 2022 Forum, AIAA Paper 2022-1599, Jan. 2022. https://doi.org/10.2514/6.2022-1599
- [14] Biegler, L. T., and Zavala, V. M., "Large-Scale Nonlinear Programming Using IPOPT: An Integrating Framework for Enterprise-Wide Optimization," *Computers and Chemical Engineering*, Vol. 33, No. 3, March 2008, pp. 575–582. https://doi.org/10.1016/j.compchemeng.2008.08.006
- [15] Patterson, M. A., Hager, W. W., and Rao, A. V., "A ph Mesh Refinement Method for Optimal Control," Optimal Control Applications and Methods, Vol. 36, No. 4, July–Aug. 2015, pp. 398–421. https://doi.org/10.1002/oca.2114
- [16] Weinstein, M. J., and Rao, A. V., "Algorithm 984: ADiGator, a Toolbox for the Algorithmic Differentiation of Mathematical Functions in MAT-LAB Using Source Transformation via Operator Overloading," ACM Transactions on Mathematical Software, Vol. 44, No. 2, Aug. 2017, pp. 1–25. https://doi.org/10.1145/3104990
- [17] Patterson, M. A., and Rao, A. V., "GPOPS-II: A MATLAB Software for Solving Multiple-Phase Optimal Control Problems Using hp-Adaptive Gaussian Quadrature Collocation Methods and Sparse Nonlinear Programming," ACM Transactions on Mathematical Software, Vol. 41, No. 1, Oct. 2014, pp. 1:1–1:37. https://doi.org/10.1145/2558904

Y. Xu Associate Editor